Kramers–Kronig relations for plasma-like permittivities and the Casimir force

2007 J. Phys. A: Math. Theor. 40 F339

(http://iopscience.iop.org/1751-8121/40/17/F04)

IOP FTC
IOP PUBLISHING JOURNAL OF PHYSICS A: MATHEMATICAL AND THEORETICAL

J. Phys. A: Math. Theor. **40** (2007) F339–F346 doi:10.1088/1751-8113/40/17/F04

FAST TRACK COMMUNICATION

Kramers–Kronig relations for plasma-like permittivities and the Casimir force

G L Klimchitskaya[1], U Mohideen[2] and V M Mostepanenko[3]

[1] North-West Technical University, Millionnaya St. 5, St. Petersburg, Russia
[2] Department of Physics and Astronomy, University of California, Riverside, CA 92521, USA
[3] Noncommercial Partnership 'Scientific Instruments', Tverskaya St. 11, Moscow, Russia

Received 26 February 2007, in final form 11 March 2007
Published 11 April 2007
Online at stacks.iop.org/JPhysA/40/F339

Abstract
The Kramers–Kronig relations are derived for the permittivity of the usual plasma model which neglects dissipation and of a generalized model which takes into account the interband transitions. The generalized plasma model is shown to be consistent with all precision experiments on the measurement of the Casimir force.

PACS numbers: 05.30.−d, 77.22.Ch, 12.20.Ds

1. Introduction

It is common knowledge that the Kramers–Kronig relations connect real and imaginary parts of an analytic function describing some causal physical process. In statistical physics and electrodynamics any material susceptibility satisfies the Kramers–Kronig relations [1, 2]. Specifically, they are used to calculate the real part of the dielectric permittivity, $\varepsilon'(\omega)$, along the real frequency axis and the dielectric permittivity, $\varepsilon(i\xi)$, along the imaginary frequency axis [2, 3]. Both are expressed through the imaginary part of the permittivity, $\varepsilon''(\omega)$, at all real frequencies.

In the last few years, the Kramers–Kronig relations have been repeatedly used to calculate the thermal Casimir force in the framework of the Lifshitz theory (see, e.g., reviews [4, 5] and recent proceedings [6]). The Casimir force [7] acts between neutral material bodies and originates from the zero-point oscillations of the electromagnetic field. The Lifshitz theory allows one to express the Casimir force at a temperature T in terms of $\varepsilon(i\xi)$ of the body materials at discrete Matsubara frequencies $\xi_l = 2\pi k_B T l/\hbar$, where k_B is the Boltzmann constant and $l = 0, 1, 2, \ldots$. The tabulated optical data for the complex index of refraction and hence for $\varepsilon''(\omega)$ are, however, available only in some restricted frequency regions [8]. Therefore, the direct calculation of $\varepsilon(i\xi)$ using the Kramers–Kronig relations is not possible and different approaches to find $\varepsilon(i\xi)$ have been proposed.

In the first approach [9, 10], the quantity $\varepsilon''(\omega)$ obtained from the tabulated optical data is extrapolated using the imaginary part of the Drude dielectric function to all lower frequencies

including zero frequency. Then $\varepsilon(i\xi_l)$ at all $l \geqslant 0$ is found from the Kramers–Kronig relations and is substituted into the Lifshitz formula at nonzero temperature. From the theoretical point of view this approach may seem straightforward, but it leads to a violation of the Nernst heat theorem for perfect crystal lattices with no impurities [11] and to contradiction with the experiment measuring the Casimir force at separations from 160 to 750 nm [12]. The second approach [12, 13] is based on the concept of the Leontovich surface impedance [2]. This approach leads to, practically, the same contributions to the Casimir force, as the first approach, at all Matsubara frequencies with $l \geqslant 1$. The contribution of the zero-frequency term is, however, different and fixed by the impedance used. As a consequence, the second approach is not applicable at separations below the plasma wavelength (equal to 137 nm for Au) where the Leontovich impedance boundary condition becomes invalid. The third approach [14, 15] does not use the tabulated optical data but employs the dielectric permittivity of the free-electron plasma model at all frequencies. Both the second and the third approaches are in agreement with thermodynamics. They are also consistent with the experiment [12] performed at separations above the plasma wavelength. However, both the second and third approaches cannot be applied in the experiment [16, 17] where measurements start at short separations of 60 nm. This experiment although performed at $T = 300$ K was found to be consistent with the Lifshitz theory at zero temperature. (The comparative analysis of all approaches is contained in [18–20].) Note that the third, plasma model approach, may seem to be in disagreement with the Kramers–Kronig relations because the dielectric permittivity of the plasma model is entirely real. In this connection, the plasma model approach has been criticized [20] for the complete neglect of dissipation. Thus, at the moment none of the theoretical approaches to the thermal Casimir force is consistent with all the available experimental information.

In the present paper, we derive the generalized Kramers–Kronig relations for the permittivities of the free-electron plasma and a plasma-like model which incorporates dissipation due to interband transitions. We demonstrate that the permittivity of the plasma model (as any function analytic in the upper half-plane) satisfies the Kramers–Kronig relations if the contribution from the pole of the second order at zero frequency is correctly taken into account. Then we compare theoretical computations of the thermal Casimir force using the free-electron plasma model and the generalized plasma model incorporating interband transitions with the zero-temperature Casimir force calculated using the tabulated optical data. We demonstrate that the theoretical results using the generalized plasma model are in good agreement with experiment. Thus currently it is the only model for the thermal Casimir force which is consistent with all measurements performed to date. We conclude with a discussion of different types of dissipation processes and their role in the theoretical description of the Casimir force.

2. Kramers–Kronig relations for plasma and plasma-like models

We consider the generalized plasma-like dielectric permittivity of the form [21]

$$\varepsilon(\omega) - 1 = A(\omega) - \frac{\omega_p^2}{\omega^2}, \tag{1}$$

where ω_p is the plasma frequency and the oscillator term

$$A(\omega) = \sum_{j=1}^{K} \frac{f_j}{\omega_j^2 - \omega^2 - \mathrm{i}g_j\omega} \tag{2}$$

takes into account the interband transitions of core electrons. Here $\omega_j \neq 0$ are the resonant frequencies of the core electrons, g_j are the respective relaxation frequencies, f_j are the

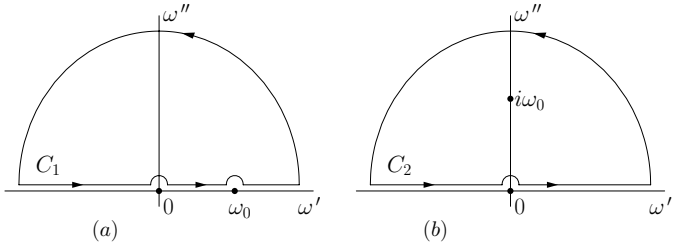

Figure 1. The integration contours (*a*) in equation (3) and (*b*) in equation (11) consisting of the real frequency axis and the semicircle of infinitely large radius.

oscillator strengths and K is the number of oscillators. The dielectric permittivity (1), (2) was used in section 7.5(D) of [21] for the description of a metal at frequencies much larger than the Drude relaxation frequency. The term $-\omega_p^2/\omega^2$ in equation (1) describes the free conduction electrons and leads to a purely imaginary current. This contribution to $\varepsilon(\omega)$ is entirely real and does not include dissipation. It must be emphasized that the oscillator term (2) does not include the oscillator with zero resonant frequency $\omega_0 = 0$. Thus it does not describe conduction electrons but only the core electrons. If the core electrons were excluded from our consideration then $f_j = 0$, $A(\omega) = 0$ and the dielectric permittivity (1) leads to the usual plasma model. Note that for the purpose of the computations below we follow the notations from [22] (Level 2, D) for the parameters of the interband oscillators. Because of this we have replaced the relaxation parameter Γ_j in [21] for g_j and the oscillator strengths $4\pi Ne^2 f_j/m$, where N is the number of molecules per unit volume, as in [21], for f_j. Here we also use $1 + A(\omega)$ in place of $\varepsilon_b(\omega)$ [21]. Equations (1) and (2) incorporate dissipation due to interband transitions but do not include processes of electron scattering on phonons, impurities, grain boundaries, surfaces and other electrons. Below we investigate the mathematical properties of equations (1), (2) for the complete frequency range from zero to infinity. The physical justification for the choice of $\varepsilon(\omega)$ in equation (1) is discussed in section 4.

The characteristic feature of the dielectric permittivity (1) is the second-order pole at zero frequency. Let us demonstrate that (1) satisfies the Kramers–Kronig relations in both cases $A(\omega) = 0$ and $A(\omega) \neq 0$. For this purpose we consider the integral

$$\int_{C_1} \frac{\varepsilon(\omega) - 1}{\omega - \omega_0}\, \mathrm{d}\omega = 0, \tag{3}$$

where ω_0 is real and the contour C_1 is presented in figure 1(*a*). Inside C_1, the function under the integral is analytic and thus the equality (3) follows from the Cauchy theorem. At infinity $\varepsilon(\omega) \to 1$ and the function $[\varepsilon(\omega) - 1]/(\omega - \omega_0)$ therefore tends to zero more rapidly than $1/\omega$. Because of this the integral along the semicircle of infinite radius is zero. We pass around the points 0 and ω_0 along the semicircles C_ρ and C_δ with radii ρ and δ, respectively. It is easily seen that

$$\int_{C_\delta} \frac{\varepsilon(\omega) - 1}{\omega - \omega_0}\, \mathrm{d}\omega = -\pi \mathrm{i}\, \mathrm{Res} \frac{\varepsilon(\omega) - 1}{\omega - \omega_0}\bigg|_{\omega=\omega_0} = -\pi \mathrm{i}[\varepsilon(\omega_0) - 1]. \tag{4}$$

The similar integral around the point 0 is more involved. Using equation (1) we represent it as a sum of the integral

$$\int_{C_\rho} \frac{A(\omega)}{\omega - \omega_0}\, \mathrm{d}\omega = -\frac{2A(0)}{\omega_0}\rho, \tag{5}$$

which vanishes when $\rho \to 0$, and

$$-\omega_p^2 \int_{C_\rho} \frac{\mathrm{d}\omega}{\omega^2(\omega-\omega_0)} \equiv \frac{\omega_p^2}{\omega_0^2} \int_{C_\rho} \left[\frac{\omega_0}{\omega^2} - \frac{1}{\omega-\omega_0} + \frac{1}{\omega}\right] \mathrm{d}\omega. \tag{6}$$

Direct integration along the semicircle C_ρ results in

$$\begin{aligned} &\int_{C_\rho} \frac{\mathrm{d}\omega}{\omega-\omega_0} = -\frac{2}{\omega_0}\rho, \qquad \int_{C_\rho} \frac{\mathrm{d}\omega}{\omega} = -\pi \mathrm{i}, \\ &\int_{C_\rho} \frac{\mathrm{d}\omega}{\omega^2} = -\frac{2}{\rho} = \omega_0 P \int_{-\infty}^{\infty} \frac{\mathrm{d}\omega}{\omega^2(\omega-\omega_0)}, \end{aligned} \tag{7}$$

where the integral is taken as a principal value. (Note that the last integral cannot be evaluated as in equation (4) because $\mathrm{Res}(1/\omega^2)|_{\omega=0} = 0$ and both integrals around the upper and lower semicircles are divergent and opposite in sign.)

Substituting equations (4)–(7) into equation (3) we arrive at

$$-\frac{\mathrm{i}\pi\omega_p^2}{\omega_0^2} - \mathrm{i}\pi[\varepsilon(\omega_0) - 1] + P\int_{-\infty}^{\infty} \frac{\mathrm{d}\omega}{\omega-\omega_0}\left[\varepsilon(\omega) - 1 + \frac{\omega_p^2}{\omega^2}\right] = 0. \tag{8}$$

Now we replace the integration variable ω by ξ, ω_0 by ω and represent the function $\varepsilon(\omega)$ in the form of $\varepsilon(\omega) = \varepsilon'(\omega) + \mathrm{i}\varepsilon''(\omega)$. Taking into account that

$$P\int_{-\infty}^{\infty} \frac{\mathrm{d}\omega}{\omega-\omega_0} = 0 \tag{9}$$

and separating the real and imaginary parts in equation (8), we obtain the generalized Kramers–Kronig relations

$$\varepsilon'(\omega) = 1 + \frac{1}{\pi} P\int_{-\infty}^{\infty} \frac{\varepsilon''(\xi)}{\xi-\omega}\,\mathrm{d}\xi - \frac{\omega_p^2}{\omega^2}, \qquad \varepsilon''(\omega) = -\frac{1}{\pi} P\int_{-\infty}^{\infty} \frac{\varepsilon'(\xi) + \frac{\omega_p^2}{\xi^2}}{\xi-\omega}\,\mathrm{d}\xi. \tag{10}$$

Note that the standard relations [2] obtained for permittivities with no pole at $\omega = 0$ do not contain terms ω_p^2/ξ^2 on the right-hand sides of equations (10).

The dielectric permittivity along the imaginary frequency axis can be determined through the use of the integral

$$\int_{C_2} \frac{\omega[\varepsilon(\omega) - 1]}{\omega^2 + \omega_0^2}\,\mathrm{d}\omega = \pi \mathrm{i}[\varepsilon(\mathrm{i}\omega_0) - 1] \tag{11}$$

along the contour C_2 in figure 1(*b*). By integrating over C_2 we get

$$\mathrm{i}\pi\frac{\omega_p^2}{\omega_0^2} + P\int_{-\infty}^{\infty} \frac{\omega\,[\varepsilon(\omega) - 1]}{\omega^2 + \omega_0^2}\,\mathrm{d}\omega = \mathrm{i}\pi[\varepsilon(\mathrm{i}\omega_0) - 1]. \tag{12}$$

Now we make the same replacement of variables as above, separate the real and imaginary parts of $\varepsilon(\omega)$ under the integral and use the identities

$$P\int_{-\infty}^{\infty} \frac{\xi\,\mathrm{d}\xi}{\xi^2 + \omega^2} = 0, \qquad P\int_{-\infty}^{\infty} \frac{\xi\varepsilon'(\xi)}{\xi^2 + \omega^2}\,\mathrm{d}\xi = 0. \tag{13}$$

The result is

$$\varepsilon(\mathrm{i}\omega) - 1 = \frac{1}{\pi} P\int_{-\infty}^{\infty} \frac{\xi\varepsilon''(\xi)}{\xi^2 + \omega^2}\,\mathrm{d}\xi + \frac{\omega_p^2}{\omega^2}. \tag{14}$$

For the usual plasma model $\varepsilon''(\omega) = 0$, $\varepsilon'(\omega) = 1 - \omega_p^2/\omega^2$, $\varepsilon(\mathrm{i}\omega) = 1 + \omega_p^2/\omega^2$, the generalized Kramers–Kronig relations (10), (14) are satisfied with the use of equation (9). In

contrast, the same plasma model violates the standard Kramers–Kronig relations. Note that sometimes [23] the plasma model is ascribed a nonzero imaginary part

$$\varepsilon''(\omega) = -\frac{\omega_p^2}{\omega}\lim_{g\to 0}\frac{1}{\omega+\mathrm{i}g} = \frac{\omega_p^2}{\omega}\pi\delta(\omega), \tag{15}$$

which is obtained from the Drude dielectric function in the limit of zero relaxation parameter. This makes it possible to formally satisfy the standard dispersion relation for the dielectric permittivity along the imaginary frequency axis [2] given by equation (14) without the ω_p^2/ω^2 term. However, the other two standard Kramers–Kronig relations with $\varepsilon''(\omega)$, as given by equation (15), become meaningless. Thus, the permittivity of the collisionless free-electron gas is entirely real.

It is easily seen that the plasma-like dielectric permittivity (1), (2) satisfies the generalized Kramers–Kronig relations (10) and (14). This can be verified by direct substitution. For example, the substitution of equations (1) and (2) into the first equation of (10) leads to

$$\begin{aligned}\sum_{j=1}^{K}\frac{f_j\left(\omega_j^2-\omega^2\right)}{\left(\omega_j^2-\omega^2\right)^2+g_j^2\omega^2} &= \frac{1}{\pi}\sum_{j=1}^{K}f_j g_j P\int_{-\infty}^{\infty}\frac{\xi\,\mathrm{d}\xi}{(\xi-\omega)\left[\left(\omega_j^2-\xi^2\right)^2+g_j^2\xi^2\right]}\\ &= \frac{1}{\pi}\sum_{j=1}^{K}\frac{f_j g_j}{\left(\omega_j^2-\omega^2\right)^2+g_j^2\omega^2}\\ &\quad\times\left[\omega_j\int_{-\infty}^{\infty}\frac{\mathrm{d}y}{y^4-2\beta_j y^2+1}-\frac{\omega^2}{\omega_j}\int_{-\infty}^{\infty}\frac{y^2\,\mathrm{d}y}{y^4-2\beta_j y^2+1}\right],\end{aligned} \tag{16}$$

where $\beta_j \equiv 1-g_j^2/\left(2\omega_j^2\right)$. When the following

$$\int_{-\infty}^{\infty}\frac{\mathrm{d}y}{y^4-2\beta_j y^2+1} = \int_{-\infty}^{\infty}\frac{y^2\,\mathrm{d}y}{y^4-2\beta_j y^2+1} = \frac{\pi}{\sqrt{2(1-\beta_j)}} \tag{17}$$

is taken into account equation (16) is satisfied. The second equation in (10) and equation (14) can be verified in a similar way.

3. Calculation of the Casimir force using the generalized plasma model and comparison with experiment

We have calculated the thermal Casimir force F^{th} acting between Au-coated test bodies in the most precise short-separation experiment [16] (a sphere of $R = 95.65\,\mu$m radius and a plate) by substituting the generalized plasma dielectric function (1), (2) into the Lifshitz formula. The Lifshitz formula for the force between a sphere and a plate was obtained by means of the proximity force approximation (PFA) as $2\pi R\mathcal{F}$ where $\mathcal{F}$ is the free energy in the configuration of two parallel plates (see [5, 17] for details). Note that recently the high accuracy of PFA was confirmed using the path-integral approach [24, 25] and worldline numerics [26]. The oscillator parameters for Au in equation (2) were found in [22, 27] using DESY data. They are as follows: $K = 3, \omega_1 = 3.87$ eV, $f_1 = 59.61\,(\mathrm{eV})^2$, $g_1 = 2.62$ eV, $\omega_2 = 8.37$ eV, $f_2 = 122.55\,(\mathrm{eV})^2$, $g_2 = 6.41$ eV, $\omega_3 = 23.46$ eV, $f_3 = 1031.19\,(\mathrm{eV})^2$, $g_3 = 27.57$ eV. Computations were performed at the laboratory temperature $T = 300$ K at different experimental separations a with $\omega_p = 9.0$ eV [8, 17]. The obtained magnitudes of the Casimir force are presented in table 1 (column 2). For comparison in column 3 we present the force magnitudes obtained using the usual plasma model of equation (1) with $A(\omega) = 0$. Column 4 lists the force magnitudes from the zero-temperature Lifshitz formula using the tabulated optical data for the complex index of refraction (recall that in [16, 17] the experimental data

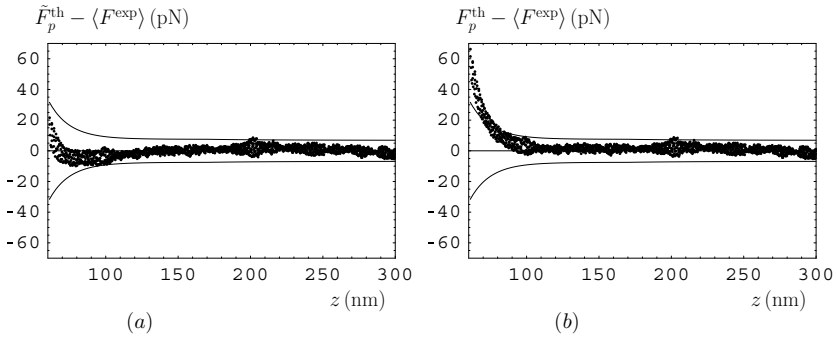

Figure 2. Differences between the theoretical and mean experimental [16] Casimir forces versus separation. Theoretical forces are computed using (*a*) the generalized plasma-like model and (*b*) the usual plasma model.

Table 1. Magnitudes of the Casimir force at different separations in column 1 computed at $T = 300$ K using the generalized plasma-like model (column 2), the usual plasma model (column 3) and at zero temperature using the tabulated optical data for the complex index of refraction (column 4).

	Force magnitude (pN)		
a (nm)	Generalized plasma model	Plasma model	Force at zero temperature
60	531.1	483.2	527.4
70	358.8	332.2	356.1
80	254.9	239.1	252.8
90	188.2	178.3	186.5
100	143.3	136.8	141.9
120	88.94	86.00	88.01
150	49.30	48.19	48.71
200	22.75	22.46	22.44
250	12.37	12.28	12.19
300	7.478	7.438	7.355

were compared with theory at zero temperature). As is seen from table 1, at short separations the results from the usual plasma model (column 3) deviate significantly from the predictions of the generalized plasma model (column 2). At the same time, the results in column 2 are in close agreement with computations at $T = 0$ (column 4) which are both consistent with experiment.

Direct comparison with the experimental data of [16] confirms that the generalized plasma model (1), (2) is consistent with measurements of the Casimir force at short separations. In figure 2(*a*), we plot the differences between the theoretical forces computed using the generalized plasma model, $\tilde{F}_p^{\rm th}$, and the mean values of the measured forces. As is seen in figure 2(*a*), almost all points are inside the error bars for the difference between theory and experiment [12, 28] computed at a 95% confidence level (solid lines). Note that the comparison of data with the zero-temperature theoretical force practically coincides with that shown in figure 2(*a*). By contrast in figure 2(*b*) the theoretical force, $F_p^{\rm th}$, is computed using the usual plasma model. It is clearly seen that at short separations the usual plasma model is inconsistent with data whereas at larger separations both models are in agreement with measurements.

Referring back to the introduction, the usual plasma model is consistent with the data of experiment [12] which is the most precise experiment at separations from 160 to 750 nm. At such large separations, the predictions of the generalized and usual plasma models almost coincide (in fact, the use of the generalized plasma model instead of the usual one leads to slightly better agreement between experiment and theory in [12]). Thus, we can conclude that the generalized plasma model (1), (2) both exactly satisfies the Kramers–Kronig relations and is also the only model consistent with all precise experiments on the Casimir force performed to date.

4. Discussion

As was mentioned in the introduction, the usual plasma model neglects the role of free-electron scattering. In the absence of scattering, the conductivity of free electrons is purely imaginary and the dielectric permittivity is completely real signifying the absence of dissipation. The generalized plasma-like dielectric permittivity (1), (2), as well as the usual plasma model, does not take into account the scattering processes of the free electrons. However, it includes dissipation due to the interband transitions of core electrons. These transitions are described by a set of oscillators with nonzero resonant frequencies. Our results demonstrate that the generalized plasma model exactly satisfies the Kramers–Kronig relations and is also consistent with all available experimental data. In the same way, as in [11, 29, 30], it can also be shown that this model is in agreement with the Nernst heat theorem.

The dissipation processes of free electrons on phonons, impurities, etc are not included in the generalized plasma model. They can be taken into account by modifying equation (1) to the form

$$\varepsilon(\omega) - 1 = A(\omega) - \frac{f_0}{\omega(\omega + \mathrm{i}g_0)}, \tag{18}$$

where $f_0 = \omega_p^2$. The second term on the right-hand side of equation (18) is the contribution of an oscillator with zero resonant frequency, $\omega_0 = 0$, which was not included in equation (2). This additional oscillator results in a first-order pole and leads to the Drude-type term in the dielectric permittivity. The Kramers–Kronig relations for the dielectric permittivity (18) are familiar [2]. However, as was discussed in the introduction, the use of the dielectric permittivity (18) leads to a violation of the Nernst heat theorem for perfect crystal lattices and to a contradiction with experiment [12]. The question why the inclusion of one type of dissipation (interband transitions of core electrons) in the Lifshitz theory is necessary while that of another (scattering processes of free electrons) leads to contradictions with fundamental physical principles and experiment remains open. Future theoretical and experimental developments will shed light on this issue.

Acknowledgments

This work was supported by the DOE Grant No DE-FG02-04ER46131. Numerical computations were supported by the NSF Grant No PHY0355092. GLK and VMM are grateful to the Department of Physics and Astronomy, University of California (Riverside) for its kind hospitality. VMM is grateful to D I Abramov for helpful discussion.

References

[1] Lifshitz E M and Pitaevskii L P 1980 *Statistical Physics* Part II (Oxford: Pergamon)
[2] Landau L D, Lifshitz E M and Pitaevskii L P 1984 *Electrodynamics of Continuous Media* (Oxford: Pergamon)

[3] Milonni P W 1994 *The Quantum Vacuum* (San Diego: Academic)
[4] Kardar M and Golestanian R 1999 *Rev. Mod. Phys.* **71** 1233
[5] Bordag M, Mohideen U and Mostepanenko V M 2001 *Phys. Rep.* **353** 1
[6] Elizalde E and Odintsov S D (ed) 2006 Papers presented at the *7th Workshop on Quantum Field Theory Under the Influence of External Conditions J. Phys. A: Math. Gen.* **39** 6109
[7] Casimir H B G 1948 *Proc. K. Ned. Akad. Wet.* **51** 793
[8] Palik E D (ed) 1985 *Handbook of Optical Constants of Solids* (New York: Academic)
[9] Boström M and Sernelius B E 2000 *Phys. Rev. Lett.* **84** 4757
[10] Brevik I, Aarseth J B, Høye J S and Milton K A 2005 *Phys. Rev.* E **71** 056101
[11] Bezerra V B, Klimchitskaya G L, Mostepanenko V M and Romero C 2004 *Phys. Rev.* A **69** 022119
[12] Decca R S, López D, Fischbach E, Klimchitskaya G L, Krause D E and Mostepanenko V M 2005 *Ann. Phys., NY* **318** 37
[13] Geyer B, Klimchitskaya G L and Mostepanenko V M 2003 *Phys. Rev.* A **67** 062102
[14] Genet C, Lambrecht A and Reynaud S 2000 *Phys. Rev.* A **62** 012110
[15] Bordag M, Geyer B, Klimchitskaya G L and Mostepanenko V M 2000 *Phys. Rev. Lett.* **85** 503
[16] Harris B W, Chen F and Mohideen U 2000 *Phys. Rev.* A **62** 052109
[17] Chen F, Klimchitskaya G L, Mohideen U and Mostepanenko V M 2004 *Phys. Rev.* A **69** 022117
[18] Bezerra V B, Decca R S, Fischbach E, Geyer B, Klimchitskaya G L, Krause D E, López D, Mostepanenko V M and Romero C 2006 *Phys. Rev.* E **73** 0281101
[19] Mostepanenko V M, Bezerra V B, Decca R S, Fischbach E, Geyer B, Klimchitskaya G L, Krause D E, López D and Romero C 2006 *J. Phys. A: Math. Gen.* **39** 6589
[20] Høye J S, Brevik I, Aarseth J B and Milton K A 2006 *J. Phys. A: Math. Gen.* **39** 6031
[21] Jackson J D 1999 *Classical Electrodynamics* (New York: Wiley)
[22] Parsegian V A 2005 *Van der Waals Forces: A Handbook for Biologists, Chemists, Engineers, and Physicists* (Cambridge: Cambridge University Press)
[23] Kittel C 1976 *Introduction to Solid State Physics* (New York: Wiley)
[24] Emig T, Jaffe R L, Kardar M and Scardicchio A 2006 *Phys. Rev. Lett.* **96** 080403
[25] Bordag M 2006 *Phys. Rev.* D **73** 125018
[26] Gies H and Klingmüller K 2006 *Phys. Rev. Lett.* **96** 220401
[27] Parsegian V A and Weiss G H 1981 *J. Colloid Interface Sci.* **81** 285
[28] Klimchitskaya G L, Chen F, Decca R S, Fischbach E, Krause D E, López D, Mohideen U and Mostepanenko V M 2006 *J. Phys. A.: Math. Gen.* **39** 6485
[29] Geyer B, Klimchitskaya G L and Mostepanenko V M 2005 *Phys. Rev.* D **72** 085009
[30] Klimchitskaya G L, Geyer B and Mostepanenko V M 2006 *J. Phys. A.: Math. Gen.* **39** 6495